ACOUSTIC TARGET STRENGTH OF FOUR MAJOR CHINESE CARPS USING THE KIRCHHOFF-RAY MODE MODEL

WAN, C. Y.[1] – ZHU, M. X.[1] – PENG, L.[1] – LI, J. Y.[1] – CAI, Z. Y.[1] – KANG, M.[2*] – ZHANG, H.[1*]

[1]*Key Laboratory of Freshwater Biodiversity Conservation, Ministry of Agriculture and Rural Affairs of China; Yangtze River Fisheries Research Institute, Chinese Academy of Fishery Sciences, Wuhan 430223, China*

[2]*Department of Maritime Police and Production System, The Institute of Marine Industry, Gyeongsang National University, Tongyeong-si, South Korea*

[*]*Corresponding authors*
e-mail: mk@gnu.ac.kr; zhanghui@yfi.ac.cn

(Received 5th May 2025; accepted 10th Jul 2025)

Abstract. The four major Chinese carps (FMCCs)—silver carp (*Hypophthalmichthys molitrix*), bighead carp (*Aristichthys nobilis*), grass carp (*Ctenopharyngodon idella*), and black carp (*Mylopharyngodon piceus*)—are among the most commercially significant freshwater fish species in China. Accurate target strength (TS) measurements are essential for acoustic stock assessments, yet reliable TS data for FMCCs remain limited. This study utilized X-ray imaging to analyze 69 specimens across the four species, generating digital representations of their swim bladders and body morphologies. The Kirchhoff-ray mode (KRM) model was applied to estimate the TS of FMCCs and its variations based on sound wave frequency, pitch angle distributions, and morphological features. Results revealed that the TS was significantly affected by the pitch angle and varied greatly with frequency, TS was the highest within a pitch angle range of 65° to 85°, and the number of secondary TS peaks increased with higher frequencies. Regression equations for TS-body length (TS-BL) relationships, as well as standard b_{20} formulations, were established for various pitch angle distributions (N[90°, 5°], N[90°, 10°], N[90°, 20°], and N[85°, 15°]) and frequencies (70, 120, 200 kHz). A comparison with previous *ex situ* experimental data highlighted some discrepancies between the results from the modeling approach and *ex situ* methods. This study provides fundamental data to support the stock assessment and species identification of FMCCs, contributing valuable insights for sustainable fisheries management.
Keywords: *fishery acoustics, frequency, freshwater fish, pitch angle, fishery resources*

Introduction

The four major Chinese carps (FMCCs)—silver carp (*Hypophthalmichthys molitrix*), bighead carp (*Aristichthys nobilis*), grass carp (*Ctenopharyngodon idella*), and black carp (*Mylopharyngodon piceus*)—are among the most important commercial freshwater fish in China. These species play a crucial role in China's economy, ecology, and dietary culture (Liu et al., 2017; Yuan et al., 2019; Xiao et al., 2022). FMCCs dominate the country's freshwater aquaculture sector and are also widely present in many natural water bodies (Yu et al., 2018). In 2022, the aquaculture production of FMCCs reached 13.8 million tons, constituting 51% of China's total freshwater fish aquaculture output (27.1 million tons) (Yu et al., 2023). These carps are widely distributed in rivers, lakes, and ponds across China. Among them, silver carp and bighead carp, which are filter-feeding species, are believed to contribute to water quality improvement and are the most commonly stocked fish in Chinese rivers and lakes (Zhang et al., 2022). However, the FMCCs, also referred to as "Asian carps" in North America, are recognized as highly invasive species outside their native range. Their introduction has caused severe economic and ecological disruptions in affected regions (Kočovský et al., 2018; Li et al.,

http://www.aloki.hu ● ISSN 1589 1623 (Print) ● ISSN 1785 0037 (Online)
DOI: http://dx.doi.org/10.15666/aeer/2305_90419054

2021; Robinson et al., 2021). Consequently, evaluating the biomass of FMCC resources in aquatic environments is essential for developing effective fishery management strategies and ensuring ecological security.

Acoustic techniques are widely recognized for their ability to cover large spatial scales efficiently, and non-invasive nature, making them an effective method for assessing the distribution and abundance of aquatic species (Koslow et al., 2009; Gastauer et al., 2017; Takakura et al., 2023; Yamamoto et al., 2023; Kang et al., 2021, 2024a). These methods are particularly valued for their non-contact and non-damaging approach to biological resources. In recent years, the application of acoustic technology has expanded to include freshwater ecosystems and aquaculture environments (Jurvelius et al., 2005; Godlewska et al., 2012; Li et al., 2024b). A critical parameter in acoustic surveys is Target Strength (TS, dB re m^2), which serves as the foundation for converting measured acoustic backscatter into biomass estimates. Inaccurate TS measurements can result in biomass estimation errors of up to 50% (Dunning et al., 2023; Li et al., 2024). Particularly, establishing a robust relationship between TS and fish length is essential for ensuring the accuracy of fish stock assessments.

Three commonly used methods for TS estimation are: (1) *in situ* measurements of free-swimming fish in their natural habitat (Cordue et al., 2001; Stevens et al., 2021); (2) *ex situ* measurements of dead or live fish in controlled environments, such as net cages (Kang et al., 2004; Johnson et al., 2019); and (3) theoretical or numerical backscattering models based on fish anatomy (Zhang et al., 2018). TS has been shown to be influenced not only by fish length but also by factors such as behavior, swimming direction, maturity status, and seasonal variations (Ona, 1990). A case study demonstrated the derivation of the TS-fish length relationship through precise *in situ* measurements of TS for rainbow smelt in freshwater environments (Rudstam et al., 2003). The *in situ* method requires specific conditions, such as discrete distribution and single-species dominance, which are challenging to meet, particularly in mixed-species environments (Tong et al., 2022). *Ex situ* measurement in controlled environments, such as cages, constrain the fish's free-swimming behavior and lack flexibility. By contrast, backscattering models enable the prediction of theoretical backscatter using precise measurements and settings, including organism anatomy, material properties, swimbladder morphology, tilt angles, and frequencies (Henderson and Horne, 2007).

FMCCs are widely distributed across China and inhabit diverse water bodies beyond its borders. Understanding the relationship between TS and factors such as fish length, acoustic frequency, and pitch angle is therefore crucial. The TS data for FMCCs can serve as a valuable reference for conducting acoustic surveys of this species across various aquatic environments. This study aimed to establish the relationship between TS and fish length for FMCCs at frequencies of 70, 120, and 200 kHz. Additionally, it analyzed the effects of swimming angle, fish morphology, and other relevant factors on TS. To evaluate the reliability of the findings in this study, further comparisons were conducted with the outcomes of previous research.

Materials and methods

Fish samples

Fish samples were obtained from several aquaculture facilities located in Hubei, Guizhou, Sichuan, and Chongqing provinces to ensure a diverse representation of fish sources. For each species, multiple samples of different body lengths from juveniles to

http://www.aloki.hu ● ISSN 1589 1623 (Print) ● ISSN 1785 0037 (Online)
DOI: http://dx.doi.org/10.15666/aeer/2305_90419054

adults were selected, including *M. piceus* (6.9 – 39.2 cm), *C. idella* (8.5 – 42.0 cm), *H. molitrix* (6.6 – 43.0 cm), and *A. nobilis* (8.6 – 46.9 cm).. The live fish were carefully transported to the laboratory under safe conditions and acclimatized in water tanks for 12 hours to adapt to their new environment.

Morphological measurements

Live fish were anesthetized using a small dose of MS-222 before measuring their total length (TL), body length (BL), and body weight (BW). X-ray imaging was performed using a Digital Radiography X-Ray Machine System for Veterinary RV-32B (maximum tube voltage: 120 kV; Dawei Veterinary Medical Co. Ltd. Jiangsu, China) to capture detailed dorsal and lateral views of the fish. In total, 69 fresh FMCCs were radiographed. *Fig. 1* displays four representative individuals from each species. The entire process, from removing the fish from the water to complete the X-ray scan, was carefully managed to ensure it did not exceed two mins. Furthermore, 2 to 3 specimens from each species were selected for dissection and detailed anatomical observation.

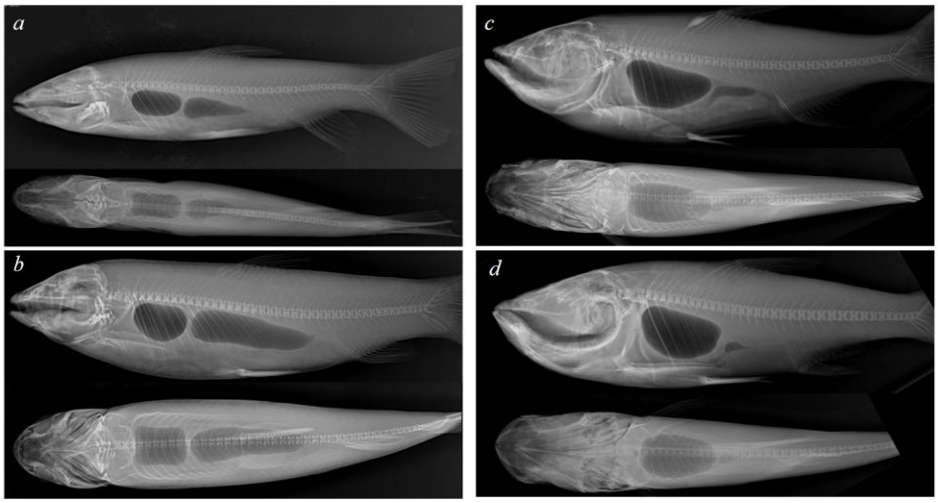

Figure 1. *X-ray images of FMCCs. a M. piceus (BL = 28.8 cm). b C. idella (BL = 37.5 cm). c H. molitrix (BL = 50.4 cm). d A. nobilis (BL = 55.9 cm)*

KRM model and data analysis

The KRM model was employed to estimate TS. This model approximates each scattering individual as an adjacent series of finite cylinders, capturing the acoustic properties of each sample (Li et al., 2024). The swimbladder was conceptualized as a set of gas-filled cylinders encased by the fish body, which can be represented as a series of fluid-filled cylinder sections. Both the fish body and swimbladder were divided into cylinders at 1 mm intervals, with their contours digitized using GetData Graph Digitizer v2.26. KRM model is implemented via the "KRMr" package in R version 4.2.1 (Gastauer, 2023). *Table 1* presents the typical parameters used in the KRM model for calculating TS (Clay and Horne, 1994). The total fish TS was calculated as the coherent sum of both the fish body and swimbladder cylindrical elements.

http://www.aloki.hu ● ISSN 1589 1623 (Print) ● ISSN 1785 0037 (Online)
DOI: http://dx.doi.org/10.15666/aeer/2305_90419054

Table 1. *Acoustic parameters used for KRM computations*

Model parameters	Values
Speed of sound in water (m/s)	1485
Speed of sound in fish body (m/s)	1575
Speed of sound in swimbladder (m/s)	345
Density of the water (kg/m^3)	1000
Density of fish body (kg/m^3)	1063
Density of the swimbladder (kg/m^3)	1.24

To investigate the variability of morphological structures in fish, the volumes of the fish body and swimbladder was determined by summing the volumes of each individual cylinder and constructing a relationship between the swimbladder volume and the body length (BL) of the fish. The total volume can be given by:

$$V = \sum_{1}^{N_S-1} \pi a_j b_j L_j \quad \text{(Eq.1)}$$

where L_j represents the jth cylinder along the fish vertebral column, a and b denote the radii of the major and minor axes, respectively, of each elliptic cylinder (Yang et al., 2023).

The TS of fish is closely related to both the sound wave frequency and the swimming pitch angle (θ). When the incident sound wave is perpendicular to the dorsal aspect of the fish body, $\theta > 90°$ indicates a head-up position, while $\theta < 90°$ indicates a head-down position. Using the KRM model, the TS of each fish was calculated over a frequency range of 20 to 200 kHz and a swimming pitch angle range of 65° to 115°, corresponding to 25° head-down and 25° head-up orientations. The average TS was determined by averaging the estimated TS values across the pitch angle (Tong et al., 2022). Pitch angle follows a normal distribution defined by $N[\theta, \text{Std}]$ where θ is the mean pitch angle and Std is the standard deviation (Furusawa et al., 1988). To align with existing studies (Lin et al., 2017; Xie et al., 2020; Palermino, 2023), we considered pitch angle distributions of N[90°, 5°], N[90°, 10°], N[90°, 20°], and N[85°, 15°].

Using the least squares method to fit the TS results with BL, we derived a formula representing the relationship between TS and BL, expressed as:

$$TS = \mathrm{m}\log(BL) + b \quad \text{(Eq.2)}$$

where m is the slope of the regression line, b is the intercept, and BL denotes body length. According to Furusawa (1988), this equation could be reformulated as:

$$TS = 20\log_{10} BL + b_{20} \quad \text{(Eq.3)}$$

where b_{20} is the intercept when m=20.

http://www.aloki.hu ● ISSN 1589 1623 (Print) ● ISSN 1785 0037 (Online)
DOI: http://dx.doi.org/10.15666/aeer/2305_90419054

Result

Morphology of FMCCs

A total of 69 fish samples were collected, representing four species: *M. piceus* (17 samples, BL range: 6.9 – 39.2 cm), *C. idella* (20 samples, BL range: 8.5 – 42.0 cm), *H. molitrix* (17 samples, BL range: 6.6 – 43.0 cm), and *A. nobilis* (15 samples, BL range: 8.6 – 46.9 cm). The size ranges of these samples are broadly representative of the individuals typically found in both aquaculture settings and natural environments. The X-ray scan images of the samples were of high clarity, enabling clear identification of the outlines of both the fish body and swimbladder. Using a three-dimensional coordinate system derived from the X-ray images, we calculated the volumes of the fish body and swimbladder for each individual. The average proportion of swimbladder volume to fish body volume was calculated for each species as follows: *M. piceus* (5.0%), *C. idella* (4.4%), *H. molitrix* (5.3%), and *A. nobilis* (4.5%). Detailed sample data are provided in *Table 2*. Scatter plots of body length versus body volume (V_{fb}) and swimbladder volume (V_{sb}) across the four species revealed power function relationships (*Fig. 2*), although these trends may be influenced by individual variations in swimbladder morphology.

Table 2. *Morphological characteristics of fish body and swimbladder in FMCCs (V_{fb} = fish body volume; Vs_b = swimbladder volume)*

Species	*M. piceus*	*C. idella*	*H. molitrix*	*A. nobilis*
Number of samples	17	20	17	15
Total length range (cm)	8.2 – 45.6	10.6 – 49.8	7.2 – 50.4	10.9 – 55.9
Body lengt range (cm)	6.9 – 39.2	8.5 – 42.0	6.6 – 43.0	8.6 – 46.9
Body weigth range (g)	5 – 980	14 – 1270	5 – 1440	11 – 1930
V_{fb} (cm^3)	4.5 – 969.2	12.4 – 1837.7	5.0 – 1768.8	11.7 – 2169.5
V_{sb} (cm^3)	0.2 – 43.0	0.4 – 113.6	0.2 – 92.4	0.4 – 113.3
Proportion	3.5% – 6.6%	2.9% – 6.2%	4.2% – 7.1%	3.5% – 5.6%

"Proportion" refers to the ratio of swimbladder volume to fish body volume

TS at various angles and frequencies

Fig. 3 illustrates the variation in total TS (TS_t), swimbladder TS (TS_s), and fish body TS (TS_f) with pitch angle for four fish individuals: *M. piceus* (BL = 23.6 cm), *C. idella* (BL = 37.5 cm), *H. molitrix* (BL = 43.0 cm), and *A. nobilis* (BL = 40.0 cm). The analysis, based on the KRM model, was conducted at incident frequencies of 70 kHz, 120 kHz, and 200 kHz. The results show that the variation in TS relative to whole fish was consistent with the variation of swimbladder TS, but not that of the body. TS was significantly affected by the pitch angle and varied greatly with frequency. The peak TS_t for all four individuals were observed between pitch angles of 65° and 85°. Additionally, as the frequency increases, the number of peaks in the TS curves also increases. Notably, the curves of TS_s and TS_t are nearly identical, indicating that the swimbladder is the primary contributor to acoustic backscattering in the fish.

http://www.aloki.hu ● ISSN 1589 1623 (Print) ● ISSN 1785 0037 (Online)
DOI: http://dx.doi.org/10.15666/aeer/2305_90419054

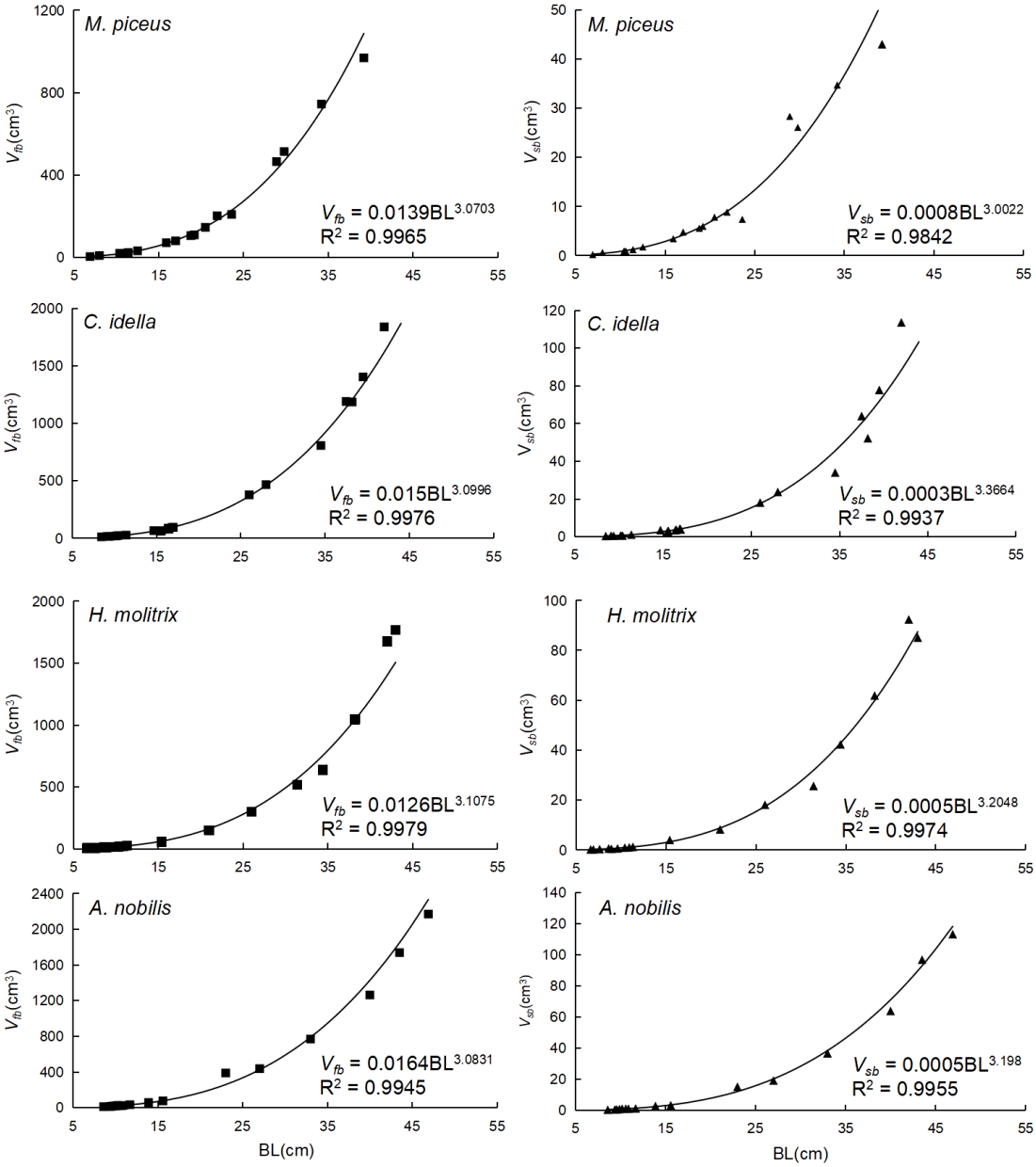

Figure 2. *Relationship among fish body volume (V_{fb}), swimbladder volume (V_{sb}) and body length (BL) across four fish species*

Average TS

Table 3 presents the average TS values for all four fish species at frequencies of 70 kHz, 120 kHz, and 200 kHz, with varying pitch angle distributions. Within the same range of pitch angles, the average TS difference among the four species at different frequencies ranges from 0.59 dB to 3.62 dB. Similarly, at the same frequency, the average TS difference among these species at different pitch angle ranges spans from 0.58 dB to 2.53 dB. This indicates that both frequency and swimming angle significantly influence TS.

http://www.aloki.hu ● ISSN 1589 1623 (Print) ● ISSN 1785 0037 (Online)
DOI: http://dx.doi.org/10.15666/aeer/2305_90419054

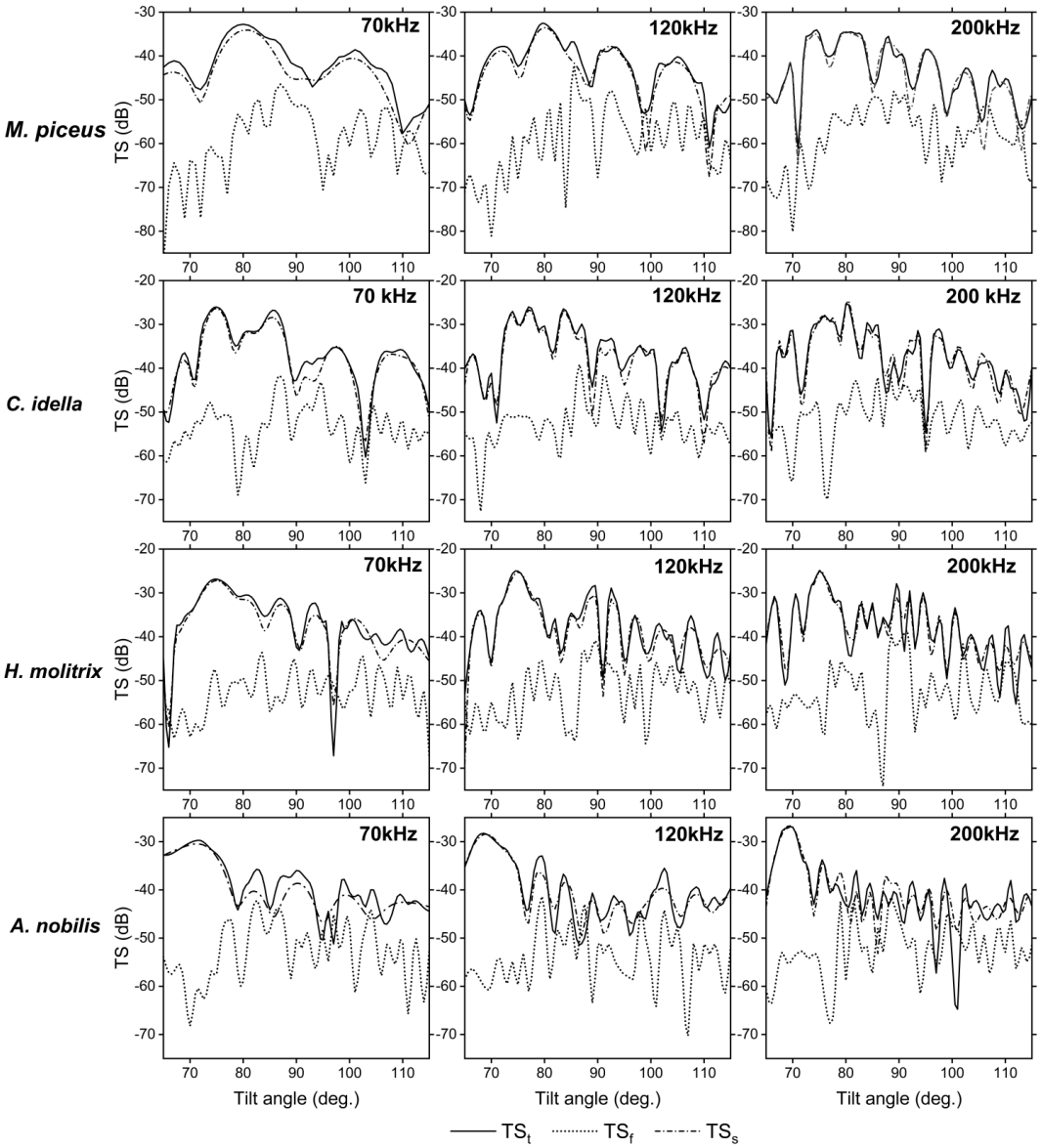

Figure 3. *Variation in TS of M. piceus (BL = 23.6 cm), C. idella (BL = 37.5 cm), H. molitrix (BL = 43.0 cm), and A. nobilis (BL = 40.0 cm) across different frequencies and incidence tilt angles. TS_t denotes the TS of the entire fish. TS_s represents the TS of the swimbladder. TS_f indicates the TS of the fish body*

TS-BL equation

C. idella was selected as a representative case to display the TS-BL relationship (*Fig. 4*) due to its largest sample size (20 specimens) and broad body length (BL) range. Meanwhile, Complete regression parameters for all species are provided in *Table 4*. The two curves in the forms of TS=mlog(BL)+b and TS=20lg(BL)+b_{20} essentially coincide. *Table 4* presents all the fitting results for the four fish species. The corresponding parameters are: *M. piceus* ($19.62 < m < 27.64$, $0.87 < r^2 < 0.96$, $-69.00 < b_{20} < -66.86$); *C. idella* ($18.60 < m < 21.57$, $0.86 < r^2 < 0.99$, $-68.38 < b_{20} < -64.85$); *H. molitrix* ($10.30 < m < 18.37$, $0.68 < r^2 < 0.94$, $-73.50 < b_{20} < -68.56$); *A. nobilis* ($18.99 < m < 25.44$, $0.78 < r^2 < 0.96$, $-72.25 < b_{20} < -67.74$).

http://www.aloki.hu ● ISSN 1589 1623 (Print) ● ISSN 1785 0037 (Online)
DOI: http://dx.doi.org/10.15666/aeer/2305_90419054

Table 3. *The average TS values for different pitch angle distributions at three frequencies*

Pitch angle distribution	Frequency (kHz)	Average TS (dB)			
		M. piceus	***C. idella***	***H. molitrix***	***A. nobilis***
N[90°, 5°]	70	−43.10	−39.71	−45.84	−45.48
	120	−42.68	−40.67	−47.76	−48.46
	200	−42.33	−40.99	−48.74	−49.10
N[90°, 10°]	70	−42.69	−40.27	−45.67	−45.36
	120	−42.88	−40.48	−47.31	−47.90
	200	−43.28	−41.09	−48.19	−48.73
N[90°, 15°]	70	−42.85	−41.8	−45.59	−45.46
	120	−43.26	−42.12	−46.78	−47.02
	200	−44.29	−43.22	−47.48	−47.82
N[85°, 15°]	70	−42.31	−40.11	−43.88	−44.04
	120	−42.69	−40.60	−45.28	−45.93
	200	−43.91	−41.38	−46.28	−46.82

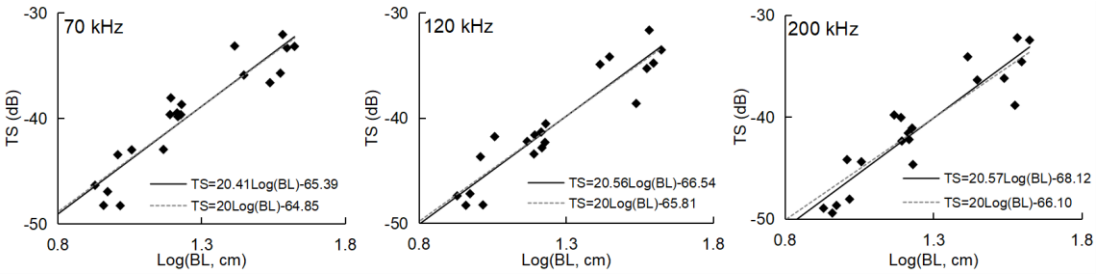

Figure 4. *The relationship between TS and BL of C. idella for pitch angle distributions N[90°, 5°]*

Table 4. *Fitting results for four fish species at different frequencies*

Species	Tilt angle (°)	TS = mlog(*BL*)+*b*											
		70kHz				120kHz				200kHz			
		m	b	r^2	b_{20}	m	b	r^2	b_{20}	m	b	r^2	b_{20}
M. piceus	*N*[90°, 5°]	27.64	−77.28	0.90	−67.55	27.51	−76.68	0.87	−67.13	21.25	−68.60	0.87	−67.00
	N[90°, 10°]	25.36	−74.04	0.95	−67.22	22.69	−70.93	0.91	−67.51	23.35	−72.13	0.94	−67.88
	N[90°, 20°]	22.00	−70.05	0.95	−67.51	19.62	−67.51	0.95	−68.00	21.47	−70.82	0.95	−69.00
	N[85°, 15°]	24.77	−72.93	0.96	−66.86	20.72	−68.31	0.93	−67.40	22.32	−71.50	0.95	−68.54
C. idella	*N*[90°, 5°]	20.41	−65.39	0.87	−64.85	21.57	−66.54	0.87	−65.81	21.57	−68.12	0.86	−66.10
	N[90°, 10°]	21.09	−66.80	0.95	−65.38	19.60	−65.12	0.95	−65.66	18.87	−64.83	0.94	−66.30
	N[90°, 20°]	20.36	−67.40	0.97	−66.95	18.60	−65.64	0.98	−67.34	20.02	−68.41	0.97	−68.38
	N[85°, 15°]	20.06	−65.34	0.98	−65.27	19.91	−65.65	0.99	−65.77	19.61	−66.06	0.97	−66.56
H. molitrix	*N*[90°, 5°]	10.30	−58.00	0.68	−70.34	12.91	−64.14	0.70	−73.17	18.37	−71.42	0.78	−73.50
	N[90°, 10°]	13.59	−61.85	0.81	−70.01	14.77	−65.85	0.79	−72.49	17.86	−70.43	0.88	−73.16
	N[90°, 20°]	16.45	−65.69	0.94	−69.95	17.43	−68.19	0.88	−71.46	16.90	−68.35	0.92	−72.29
	N[85°, 15°]	16.13	−63.63	0.88	−68.56	15.72	−65.03	0.75	−70.48	16.33	−66.67	0.84	−71.34
A. nobilis	*N*[90°, 5°]	18.99	−68.52	0.79	−69.81	22.03	−74.81	0.78	−71.50	25.64	−79.38	0.85	−72.25
	N[90°, 10°]	19.93	−69.48	0.86	−69.57	22.54	−74,25	0.87	−71.03	25.23	−78.36	0.93	−71.72
	N[90°, 20°]	20.51	−70.09	0.94	−69.45	22.14	−72.13	0.90	−70.52	22.83	−74.86	0.96	−71.18
	N[85°, 15°]	20.47	−68.31	0.93	−67.74	21.92	−71.47	0.90	−69.04	23.39	−74.22	0.94	−69.94

http://www.aloki.hu ● ISSN 1589 1623 (Print) ● ISSN 1785 0037 (Online)
DOI: http://dx.doi.org/10.15666/aeer/2305_90419054

Discussion

To use the KRM model for calculating TS, it is essential to measure specific morphological parameters of both the fish body and the swimbladder accurately. This allows for constructing the three-dimensional spatial coordinates of the fish. Therefore, the X-ray images must precisely reflect the true internal structure of the fish. For dead or frozen fish, the morphology of the swimbladder can change significantly. Hence, we opted to take X-ray images of live fish, ensuring the entire process from removing the fish from water to completing the X-ray imaging did not exceed two mins. This ensures the X-ray images closely reflect the true internal structure of the fish as it is in water. It has been suggested that slice thickness affects the accuracy of KRM results (Macaulay et al., 2013; Jech et al., 2015). Palermino (2023) compared the effects of different cylinder thicknesses on KRM results and found that a thickness of 2 mm is inappropriate, while 1 mm yields good results. However, opting for thinner slices is time-consuming and labor-intensive.

The relationship equations between TS and BL for fish, derived through modeling methods, are seldom used directly for biomass assessments in fish stock surveys. Instead, they are primarily utilized for comparison with *in situ* or *ex situ* experimental results. The FMCCs represent the most commonly found fish species in China, and numerous studies have examined their TS. *Table 5* presents a comparison between the results of this study and previous research. Moreover, to facilitate a comparison of methodologies, we have included TS-TL equations for two other fish species: *Larimichthys polyactis* and *Scomber colias*. Notably, the equations derived from modeling methods exhibit differences of 2 to 3 dB, or even greater, when compared to those derived from *ex situ* methods (caged or tethered fish). Several factors may contribute to these discrepancies: (1) variations in the number and specifications of samples selected for formula fitting; (2) differences between the selected range of pitch angles and the actual swimming angles of fish within net cages. To determine the actual distribution probability of fish swimming angles in their natural habitat, Yoon (2023) employed underwater cameras to ascertain the swimming angle range of *Larimichthys polyactis* as N[86.8°, 21.9°]. The TS-TL equations obtained through modeling methods and *ex situ* net cage methods also exhibited a variance of approximately 2 dB.

Table 5. *Comparison of equations for TS-BL/TL relationships in fish using different methods*

Species	Method	Frequency	Tilt angle (°)	TS-BL/TL relationship	Reference
C. idella	tethered	199	N[90°, 10°]	TS=20.9lg(TL)−63.40	Lin et al., 2017
	KRM	200	N[90°, 10°]	TS=20lg(TL)−66.30	this study
H. molitrix	caged	199	/	TS=19.6lg(BL)−66.50	Xie et al., 2020
	KRM	200	N[85°, 15°]	TS=20lg(BL)−68.56	this study
A. nobilis	caged	200	/	TS=22.87lg(BL)−84.50	Ren et al., 2011
	tethered	120	/	TS=35.9lg(TL)−90.30	Chen et al., 2019
Larimichthys polyactis	caged	120	/	TS=20lg(TL)−68.62	Yoon et al., 2023
	KRM	120	N[86.8°, 21.9°]	TS=20lg(TL)−66.27	
Scomber colias	caged	38	/	TS=20lg(TL)−71.60	Palermino et al., 2021
	KRM	38	N[90°, 5°]	TS=20lg(TL)−66.00	Palermino et al., 2023

Note: adjust all angle descriptions are consistent with those used in this study

http://www.aloki.hu ● ISSN 1589 1623 (Print) ● ISSN 1785 0037 (Online)
DOI: http://dx.doi.org/10.15666/aeer/2305_90419054

Several factors influence the TS of fish, including body length, frequency, and swimming angle. This study, along with numerous previous studies, suggests that the swimbladder is the predominant contributor to acoustic backscattering in fish, accounting for over 90% of the effect. Consequently, factors affecting the swimbladder's shape and size—such as dietary condition, gonad development, and its position within the water column—significantly impact the TS of fish (Tong et al., 2022; Yoon et al., 2023; Li et al., 2024). Considerable individual variability may occur within species. *Fig. 5* illustrates the differential growth rates of the fish's body and swimbladder volume relative to increases in body length. Through X-ray imaging and dissection, it was determined that both *M. piceus* and *C. idella* exhibit two swimbladders each. Conversely, in *H. molitrix* and *A. nobilis*, individual variations exist, with some possessing a single swimbladder while others have two. Moreover, the number of swimbladders appears uncorrelated with the fish's developmental stage, indicating that fish of both large and small sizes may have only one swimbladder chamber. It becomes evident that fish of identical body length but differing swimbladder quantities will exhibit variations in TS.

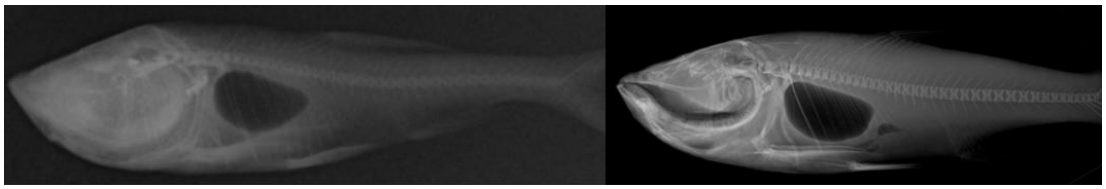

Figure 5. *Two A. nobilis specimens with different numbers of swimbladders (left: BL = 9.4 cm; right: BL = 46.9 cm)*

The swimming angle is a critical factor influencing TS. Fish exhibit varying pitch angles due to differences in body size, swimming speed, and environmental conditions. In this study, four pitch angle distributions were used to calculate the TS of FMCCs. The results reveal significant differences in TS values derived from the various angular distributions, which also diverge from those obtained in previous studies using the *ex situ* approach (Ren et al., 2011; Lin et al., 2017; Chen et al., 2019; Xie et al., 2020). Measurements of fish weight and volume indicate that the average density of all four species is less than 1 g/cm³. This buoyancy enables FMCCs to remain suspended in the water without frequently tilting their bodies to maintain depth. Consequently, selecting a narrower range of pitch angles may better represent actual conditions. However, in the absence of field measurements to validate these findings, the results are less suitable for direct application to fish stock assessments.

Based on X-ray imaging and the KRM model, this study systematically obtained the cross-frequency acoustic TS spectra of the four major Chinese carps, and established quantitative TS-BL equations under four typical pitch angle distributions. In recent years, the application of broadband techniques to identify and classify species in echograms has become a prominent focus in fishery acoustics (Yan et al., 2020; Tong et al., 2022; Kang et al., 2024b). The coupled application of the KRM model and broadband acoustic systems offers significant advantages: by collecting cross-frequency TS spectra through broadband acoustic equipment and leveraging the unique TS spectral characteristics of FMCCs modeled in this study (such as secondary peaks varying with frequency), it becomes feasible to distinguish FMCCs from coexisting

http://www.aloki.hu ● ISSN 1589 1623 (Print) ● ISSN 1785 0037 (Online)
DOI: http://dx.doi.org/10.15666/aeer/2305_90419054

species in real time. Meanwhile, combining machine learning algorithms can further improve the classification accuracy. The accuracy of TS-BL equations is the core of fish resource assessment, and the dynamic distribution of fish pitch angles in natural habitats is a key calibration parameter. Combining underwater cameras or acoustic telemetry technology to record the real-time orientation of fish in natural habitats for calibrating the KRM model can reduce uncertainties caused by static laboratory assumptions. For example, Yoon (2023) used cameras to obtain the pitch angle distribution of *Larimichthys polyactis* as N[86.8°, 21.9°]. The KRM model offers notable advantages, including minimal sample requirements, efficiency in terms of time and labor. Nonetheless, measuring TS in fish presents numerous challenges, such as variability in swimming pitch angles among species, morphological differences between individuals, and the influence of environmental factors, diurnal cycles, and seasonal changes on TS (Clay and Horne, 1992; Lloret-Lloret et al., 2020; Yang et al., 2023). Many aspects remain unknown, making them key areas for future research.

Conclusion

This study systematically quantifies the acoustic target strength (TS) characteristics of the four major Chinese carps (FMCCs) by integrating the Kirchhoff-ray mode (KRM) model with X-ray imaging. The swimbladder is confirmed as the dominant source of acoustic scattering in FMCCs (contributing over 90% to TS). TS shows significant sensitivity to pitch angle, peaking within the range of 65° to 85°, and the number of secondary peaks in the TS curve increases notably with the elevation of acoustic frequency (70 to 200 kHz). Morphological analysis further reveals that both body volume and swimbladder volume exhibit power-law correlations with body length, providing a morphological foundation for acoustic modeling.

The standardized TS-BL equations established based on the KRM model cover frequency ranges of 70, 120, and 200 kHz, as well as four pitch angle distributions. The spectral characteristics of TS across frequencies and pitch angles offer critical references for in situ species identification.

The study has limitations in the lack of in situ measurement validation. Future research should incorporate acoustic telemetry to verify the dynamic effects of pitch angle variations and environmental factors (such as temperature and salinity) on TS in natural environments, so as to enhance the universality of TS-BL equations and provide more precise technical support for FMCC resource assessment and invasive species control.

Acknowledgements. This research was supported by the Natural Science Foundation of Hubei Province, China-Temporal and spatial patterns of natural breeding populations of critically endangered Chinese sturgeons and their environmental driving mechanisms (2022CFA058) and Special project for normalized monitoring after the ban on fishing in the Yangtze River (CJJC-2024-06).

REFERENCES

[1] Chen, X., Lian, Y., Huang, G., Xiang, T., Zhang, T., Liu, J., Ye, S., Li, Z. (2019): The experimental design and application of hydroacoustical techniques for target strength of two commercial cyprinidae fish species. – Acta Hydrobiologica Sinica 43: 854-860.

http://www.aloki.hu ● ISSN 1589 1623 (Print) ● ISSN 1785 0037 (Online)
DOI: http://dx.doi.org/10.15666/aeer/2305_90419054

[2] Clay, C. S., Horne, J. K. (1994): Acoustic models of fish: The Atlantic cod (*Gadus morhua*). – The Journal of the Acoustical Society of America 96(3): 1661-1668.
[3] Cordue, P. L., Coombs, R. F., Macaulay, G. J. (2001): A least squares method of estimating length to target strength relationships from in situ target strength distributions and length frequencies. – The Journal of the Acoustical Society of America 109: 155-163.
[4] Dunning, J., Jansen, T., Fenwick, A. J., Fernandes, P. G. (2023): A new in-situ method to estimate fish target strength reveals high variability in broadband measurements. – Fisheries Research 261: 106611.
[5] Furusawa, M. (1988): Prolate spheroidal models for predicting general trends of fish target strength. – Journal of the Acoustical Society of Japan (E) 9: 13-24.
[6] Gastauer, S., Scoulding, B., Parsons, M. (2017): Estimates of variability of goldband snapper target strength and biomass in three fishing regions within the northern demersal scalefish fishery (Western Australia). – Fisheries Research 193: 250-262.
[7] Gastauer, S. (2023): KRMr: kirchhoff ray mode model for fisheries acoustics. – R package version 0.3.0. Zenodo, 0.4.6. https://github.com/SvenGastauer/KRMr.
[8] Godlewska, M., Frouzova, J., Kubecka, J., Wiśniewolski, W., Szlakowski, J. (2012): Comparison of hydroacoustic estimates with fish census in shallow Malta Reservoir-which TS/L regression to use in horizontal beam applications? – Fisheries Research 123-124: 90-97.
[9] Henderson, M. J., Horne, J. K. (2007): Comparison of in situ, Ex situ, and Backscatter Model Estimates of Pacific Hake (*Merluccius productus*) target strength. – Canadian Journal of Fisheries and Aquatic Sciences 64(12): 1781-1794.
[10] Jech, J. M., Horne, J. K., Chu, D., Demer, D. A., Francis, D. T., Gorska, N., Jones, B., Lavery, A. C., Stanton, T. K., Macaulay, G. J., Reeder, D. B., Sawada, K. (2015): Comparisons among ten models of acoustic backscattering used in aquatic ecosystem research. – The Journal of the Acoustical Society of America 138: 3742-3764.
[11] Johnson, G. R., Shoup, D. E., Boswell, K. M. (2019): Incorporating fish orientation into target strength-total length equations: Horizontal-Aspect target-strength equations for Gizzard Shad *Dorosoma cepedianum*. – Fisheries Research 218: 155-165.
[12] Jurvelius, J., Auvinen, H., Kolari, I., Marjomäki, T. J. (2005): Density and biomass of smelt (*Osmerus eperlanus*) in five Finnish lakes. – Fisheries Research 73(3): 353-361.
[13] Kang, D., Sadayasu, K., Mukai, T., Iida, K., Hwang, D., Sawada, K., Miyashita, K. (2004): Target strength estimation of black Porgy *Acanthopagrus schlegeli* using acoustic measurements and a scattering model. – Fisheries Science 70(5): 819-828.
[14] Kang, M., Kang, J. H., Kim, M., Nam, S. H., Choi, Y., Kang, D. J. (2021): Sound scattering layers within and beyond the Seychelles-Chagos Thermocline Ridge in the Southwestern Indian Ocean. – Frontiers in Marine Science 8: 769414.
[15] Kang, M., Oh, S., Oh, W., Kang, D. J., Nam, S. H., Lee, K. (2024a): Acoustic characterization of fish and macroplankton communities in the Seychelles-Chagos Thermocline Ridge of the southwest Indian ocean. – Deep Sea Research Part II: Topical Studies in Oceanography 213: 105356.
[16] Kang, M., Kim, H., Kang, D., Jung, J., Simanungkalit, F., Kang, D. (2024b): Ex situ combined in situ target strength of Japanese horse mackerel using a broadband echosounder. – Journal of the Korean Society of Fisheries and Ocean Technology 60(2): 142-151.
[17] Kočovský, P. M., Chapman, D. C., Qian, S. (2018): "Asian carp" is societally and scientifically problematic. Let's replace it. – Fisheries 43: 311-316.
[18] Koslow, J. A. (2009): The role of acoustics in ecosystem-based fishery management. – ICES Journal of Marine Science 66: 966-973.
[19] Li, D., Prinyawiwatkul, W., Tan, Y., Luo, Y., Hong, H. (2021): Asian carp: A threat to American lakes, a feast on Chinese tables. – Comprehensive Reviews in Food Science and Food Safety 20: 2968-2990.

http://www.aloki.hu ● ISSN 1589 1623 (Print) ● ISSN 1785 0037 (Online)
DOI: http://dx.doi.org/10.15666/aeer/2305_90419054

[20] Li, B., Liu, J., Gao, X., Huang, H., Wang, F., Huang, Z. (2024a): Acoustic target strength of thornfish (*Terapon jarbua*) based on the Kirchhoff-Ray mode model. – Electronics 13(7): 1279.
[21] Li, D., Du, Z., Wang, Q., Wang, J., Du, L. (2024b): Recent advances in acoustic technology for aquaculture: A Review. – Reviews in Aquaculture 16: 357-381.
[22] Lin, D., Zhang, H., Li, J., Yang, H., Di, J., Wei, Q. (2017): Target strength of four freshwater cultured fish species and a variance analysis. – Journal of Fishery Sciences of China 24: 1-10.
[23] Liu, X., Steele, J. C., Meng, X-Z. (2017): Usage, residue, and human health risk of antibiotics in Chinese aquaculture: A Review. – Environmental Pollution 223: 161-169.
[24] Lloret-Lloret, E., Navarro, J., Giménez, J., López, N., Albo-Puigserver, M., Pennino, M. G., Coll, M. (2020): The seasonal distribution of a highly commercial fish is related to ontogenetic changes in its feeding strategy. – Frontiers in Marine Science 7: 1068.
[25] Macaulay, G. J., Peña, H., Fässler, S. M., Pedersen, G., Ona, E. (2013): Accuracy of the Kirchhoff-approximation and Kirchhoff-ray-mode fish swimbladder acoustic scattering models. – PLoS ONE 8: e64055.
[26] Ona, E. (1990): Physiological factors causing natural variations in acoustic target strength of fish. – Journal of the Marine Biological Association of the United Kingdom 70: 107-127.
[27] Palermino, A., De Felice, A., Canduci, G., Biagiotti, I., Costantini, I., Centurelli, M., Leonori, I. (2023): Application of an analytical approach to characterize the target strength of ancillary pelagic fish species. – Scientific Reports 13: 15182.
[28] Ren, Y., Wang, K., Duan, X., Yin, S., Li, S., Liu, S., Chen, D. (2011): In situ hydroacoustic estimates of the target strength and behavior characteristics of *Aristichthys nobilis*. – Freshwater Fisheries 41: 3-9.
[29] Robinson, K. F., Alsip, P. J., Drake, A. R., Kao, Y., Koops, M. A., Mason, D. M., Rutherford, E. S., Zhang, H. (2021): Reviewing uncertainty in Bioenergetics and food web models to project invasion impacts: Four major Chinese carps in the Great Lakes. – Journal of Great Lakes Research 47: 83-95.
[30] Rudstam, L. G., Parker, S. L., Einhouse, D. W., Witzel, L. D., Warner, D. M., Stritzel, J. L., Parrish, D. L., Sullivan, P. J. (2003): Application of in situ target-strength estimations in lakes: Examples from rainbow-smelt surveys in lakes Erie and Champlain. – ICES Journal of Marine Science 60: 500-507.
[31] Stevens, J. R., Jech, J. M., Zydlewski, G. B., Brady, D. C. (2021): Estimating target strength of estuarine pelagic fish assemblages using fisheries survey data. – The Journal of the Acoustical Society of America 150(4): 2553-2565.
[32] Takakura, R., Tanida, K., Inazaki, A., Mitsunaga, Y. (2023): Behavioral study of black sea bream *Acanthopagrus schlegelii* by acoustic telemetry to guide countermeasures against feeding damage to cultivated nori *Neopyropia yezoensis* off Kobe, Hyogo, Japan. – Fisheries Science 89: 785-799.
[33] Tong, J., Xue, M., Zhu, Z., Wang, W., Tian, S. (2022): Impacts of morphological characteristics on target strength of chub mackerel (*Scomber japonicus*) in the Northwest Pacific Ocean. – Frontiers in Marine Science 9: 856483.
[34] Xiao, Y., Deng, J., Yang, S., Hu, J., Wang, L., Li, W. (2022): Study on the spawning habitat suitability of four major Chinese carps in the fluctuating backwater area of the Three Gorges Reservoir. – Ecological Indicators 143: 109314.
[35] Xie, X., Zhang, H., Sun, L., Cai, Z., Wang, H., Huo, L., Wei, Q. (2020): Target strength of four freshwater fish species in the Yangtze River based on cage and model method. – Journal of Fishery Sciences of China 27: 536-546.
[36] Yamamoto, N., Amakasu, K., Abe, K., Matsukura, R., Imaizumi, T., Matsuura, T., Murase, H. (2023): Volume backscattering spectra measurements of Antarctic krill using a broadband echosounder. – Fisheries Science 89: 301-315.

http://www.aloki.hu ● ISSN 1589 1623 (Print) ● ISSN 1785 0037 (Online)
DOI: http://dx.doi.org/10.15666/aeer/2305_90419054

[37] Yan, N., Mukai, T., Yamamoto, J., Hasegawa, K. (2020): Acoustic discrimination between juvenile walleye pollock and pointhead flounder. – Fisheries Research 224: 105434.
[38] Yang, Y., Gastauer, S., Proud, R., Mangeni-Sande, R., Everson, I., Kayanda, R. J., Brierley, A. S. (2023): Modelling and in situ observation of broadband acoustic scattering from the Silver Cyprinid (*Rastrineobola argentea*) in Lake Victoria, East Africa. – ICES Journal of Marine Science 81(7): 1385-1398.
[39] Yoon, E., Lee, H., Park, C., Lee, Y-D., Hwang, K., Kim, D. N. (2023): Ex situ target strength of yellow croaker (*Larimichthys polyactis*) in a seawater tank. – Fisheries Research 260: 106610.
[40] Yu, L., Lin, J., Chen, D., Duan, X., Peng, Q., Liu, S. (2018): Ecological flow assessment to improve the spawning habitat for the four major species of carp of the Yangtze River: A study on habitat suitability based on ultrasonic telemetry. – Water 10: 600.
[41] Yu, X. J., Xu, L. J., Wu, F. X. (2023): China fishery statistical yearbook in 2023. – China Agriculture Press, Beijing, pp 17-36.
[42] Yuan, L., Wang, L., Li, Z., Zhang, M., Shao, W., Sheng, G. (2019): Antibiotic resistance and microbiota in the gut of Chinese four major freshwater carp from retail markets. – Environmental Pollution 255: 113327.
[43] Zhang, H., Li, J., Wang, C., Wang, C., Wu, J., Du, H., Wei, Q., Kang, M. (2018): Acoustic target strength of the endangered Chinese sturgeon (*Acipenser sinensis*) by ex situ measurements and theoretical calculations. – Applied Sciences 8: 2554.
[44] Zhang, Z., Shi, Y., Zhang, J., Liu, Q. (2022): Experimental observation on the effects of bighead carp (*Hypophthalmichthys nobilis*) on the plankton and water quality in ponds. – Environmental Science and Pollution Research 29: 56658-56675.

http://www.aloki.hu ● ISSN 1589 1623 (Print) ● ISSN 1785 0037 (Online)
DOI: http://dx.doi.org/10.15666/aeer/2305_90419054